Chapter 6

Uncontrolled field evaluation using NDT techniques

6.1. Introduction

The earlier chapters facilitated to gain insight on assessing the structural deficiency caused by delamination in pavements and bridges using Infrared Thermography (IRT) and Ground-Penetrating Radar (GPR). The efficacy of these Non-Destructive Testing (NDT) techniques are also assessed under controlled field conditions. Pertaining to the other objectives of the study that aim to address decision-problems related to pavement prioritization projects and its inherent budgetary constraints, diligent and robust decision-support system is to be devised. In order to develop and demonstrate the decision-support framework, a case study on airfield pavements was taken, since the prioritization problem prevails for airfield pavements as well (Hajek et al., 2011). The prerequisite is the knowledge about the pavement condition in terms of measuring diverse decisive parameters, for which uncontrolled field evaluations were conducted. It may be noted that this chapter only discusses the details of the data collection process and its analysis. The devised approaches have been presented in Chapter 7.

The uncontrolled field evaluations on airfield pavements for structural condition assessment and estimation of layer thicknesses were conducted by NDT technologies namely, Heavy Weight Deflectometer (HWD) and GPR, with the help of Aimil Ltd., New Delhi. In addition to this, visual surveys were conducted to identify the types of distresses present on the pavement surfaces which were quantified using Pavement Condition Index (PCI). Visual surveys offer the identification of various distress types of pavement surface, and the distress density estimation to eventually assign a condition index, such as PCI. These surveys helped to ascertain the areas with major distresses, and deterioration, where further testing using NDT devices could be performed, and more appropriate methods of pavement rehabilitation could be implemented. HWD is deflection-based structural capacity assessment equipment, suitable for thicker pavements, such as airfield pavements. GPR is the tool based on the propagation of electromagnetic (EM) waves and

analyzing the information carried by the reflected waves. More details about these equipment have been discussed in Chapter 2.

Although a number of NDT technologies have been used on pavements worldwide, the tests performed under the study were limited to the availability of testing equipment, scope of work and time constraints. This chapter presents the testing details, and results of field investigations using the NDT technologies and discusses their advantages and limitations.

6.2. Study area

The airfield pavement network of the international airport taken as a case study in this thesis consisted of a single runway, a parallel taxiway, five exit taxiways, an international and a domestic apron. The pavement composition of runway, and taxiways included asphalt concrete surface and binder (base) courses, crushed aggregate base course and granular sub-base course over selected fill, type subgrade. This study has been performed on the runway, parallel taxiway and three Exit Taxiways (ET2, ET3, ET5). The runway was 3.05 km long, 60 m wide, and oriented as '02/20' of the airport. Figure 6.1 shows the study site with the runway, parallel taxiway, and exit taxiways (ET1 to ET5) of the airfield pavement network.

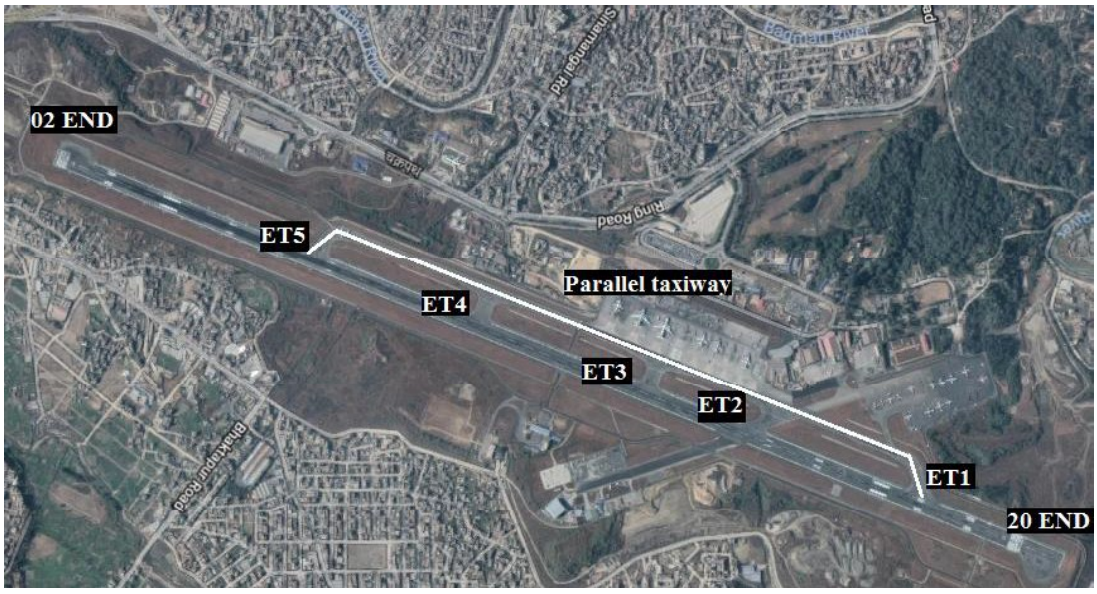

Figure 6.1. Study area showing runway and taxiways at an international airport

6.3. Visual surveys

Visual survey of the runway was conducted by a team of experts in this study, along with inspection of turn pad (02 end and 20 end), parallel taxiway, and exit taxiway (ET2, ET3 and ET5). During these surveys, various distresses with their severities and quantities were observed on the pavement surface, and facilitated the estimation of PCI. The condition index PCI can have any value between 0 (failed) to 100 (excellent) (ASTM D5340-12, 2012). The overall pavement performance can be assessed by periodically observing the rate of increase in distress density. Although PCI does not provide a direct measure of structural or functional performance of pavement but indirectly designates structural integrity and operational conditions. Hence, it offers an important basis for determining Maintenance and Rehabilitation (M&R) needs and priorities. Identification and documentation of all distress types present on the existing pavement surface were performed following ASTM standards (ASTM D5340-12, 2012). The detailed observations are discussed in the following paragraphs.

6.3.1. Runway Pavement

The existing runway surface was found to be in the variable state as seen from the results of the visual survey. An area around 35 m × 20 m between 0.025 km and 0.060 km covering almost 35% of the turn pad, showed depressions and deformations, caused particularly by shearing action of aircraft turning movements. Area from 0.05 km to 1.80 km was in fair condition with few corrugations and block cracks. The runway around exit taxiway ET4 intersection (1.80 km to 2.00 km) seemed to be in fair condition with patching and depressions at some places. Fatigue cracks have been observed to predominate area from 2.25 km to 2.50 km. Raveling and material loss have also been observed at the cracked areas. The touch-down zone (2.60 km to 2.90 km) from runway direction '02' was recognized to be severely distressed and damaged. This area has been exposed to a majority of landings by heavy commercial airlines, which impart their effect on pavement condition. At 2.87 km, the distress severity has been found to decrease. Heavy rubber deposition was found which made the surface glossy and reduced skid resistance.

Figure 6.2 shows actual images of distresses present on runway, which were observed during the visual inspection.

(a) Patching on runway

(b) Cracks on runway

(c) Rubber deposition on runway

Figure 6.2. Observations from visual inspection of runway

6.3.2. Taxiway

The study covered a survey of parallel taxiway (0.200 km to 1.825 km), exit taxiway ET2 (reference centerline location is at 0.925 km of runway), exit taxiway ET3 (reference centerline location is at 1.260 of runway), and exit taxiway ET5 (taken between 1.825 km and 1.955 km at runway edge line).

6.3.2.1. Parallel taxiway

Parts of parallel taxiway surface (especially from 0.200 to 0.250 km; 0.300 to 0.400 km; at 1.125 km in front of the international apron) were found to be heavily distressed. The deterioration in some of these portions is the maximum among the entire runway and taxiway pavements. The heavily distressed sections contained deep depressions, wide alligator cracks with varying degree of raveling, and potholes, whereas narrow to wide interconnected cracks with minor raveling characterized the surface condition of moderately distressed sections. Low to very low distressed sections were marked by the presence of localized line and interconnected alligator cracks. It appeared to be caused by localized settlement or poor subgrade condition. Longitudinal joint crack was seen to extend from 0.60 km to 1.06 km, whereas the block cracks were observed from 0.70 km to 0.94 km. Water pooling was seen along various parts of the parallel taxiway including at the turn of exit taxiway ET3. These portions required major repair/rehabilitation.

6.3.2.2. Exit taxiway ET2

The pavement surface was observed to be in fair condition except for localized distress like narrow interconnected alligator cracks and raveling.

6.3.2.3. Exit taxiway ET3

Due to its central location with the international apron, it is mostly used for taxing large aircraft. This taxiway was found to be relatively more distressed and depressions, cracks and raveling were observed.

6.3.2.4. Exit taxiway ET5

This taxiway was observed to be in poor condition. A joint reflection crack prevailed along shoulder widening. The surface was generally marked by narrow interconnected alligator cracks, depression and bleeding. Figure 6.3 shows actual images of distresses present on parallel, and exit taxiways observed during the visual inspection.

(a) Pothole on exit taxiway ET2

(b) Rutting on exit taxiway ET2

(c) Raveling on exit taxiway ET3

(d) Bleeding on exit taxiway ET5

Figure 6.3. Observations from visual inspection of taxiways

Figure 6.4 presents the area-wise distribution of pavement surface condition of runway and taxiways, respectively, based on the results of visual inspections. It can be seen that 40% area of the runway was in very poor condition, and 20% area was in poor condition. The area in fair condition is 20% of the total area that would eventually advance to the poor condition due to its continual deterioration if left unattended. Remaining 15% and 5% of the area were rated as good and very good, respectively. In the case of taxiways, 40% of the area was in very poor condition and 30% was in poor condition, which showed that 70% of the area was already deteriorated. Around 10% of the surface was rated as fair, another 10% as good, and the remaining 10% as very good.

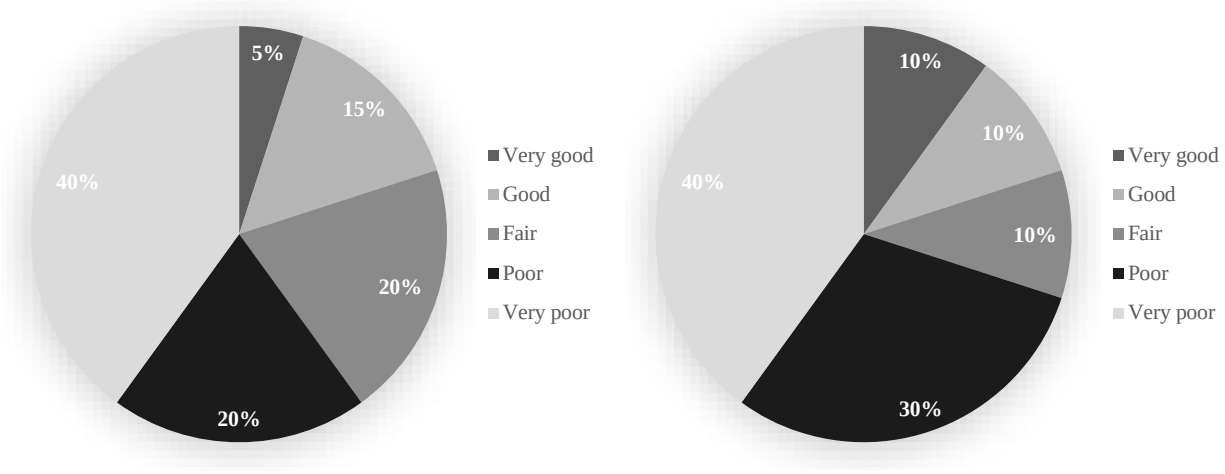

(a) Runway **(b) Taxiways**

Figure 6.4. Area-wise distribution of pavement surface condition rating

Table 6.1 summarizes the overall condition of all the pavement types in the airfield. Turn pads and parallel taxiway were in very poor condition. Runway, ET3 and ET5 were in poor condition. Only ET2 was found to be in fair condition. On the basis of these surface condition ratings, it can be concluded that the entire airfield pavement network is poor. Therefore, further testing using HWD was performed and sub-soil investigation was carried out by taking core samples at limited sites.

Table 6.1. Overall condition of various airfield pavements

Airfield pavement facility type	Overall condition
Runway	Poor
Parallel taxiway	Very poor
Exit taxiway 2	Fair
Exit taxiway 3	Poor
Exit taxiway 5	Poor
Turn pad 20	Very poor
Turn pad 02	Very poor

6.4. HWD testing

Mechanistic-empirical analysis and design methods involve the estimation of pavement layer moduli. The accurate determination of non-linear and visco-elastic stress-strain response requires heavy wheel load and precise deflection measurements. This task is facilitated by HWD tests, for its application in airfield pavements. HWD works on similar principles like Falling Weight Deflectometer (FWD), except that it consists of heavy loads for thicker pavements. The test results in the form of raw deflection data indicate the strength of airfield pavement, with large deflections indicating poor strength at the test location.

6.4.1. Instrument

Dynatest model 8081 HWD is a trailer-mounted device, and it has been used in this study to perform deflection testing over thick pavements including runways and taxiways. HWD has a loading range of 30-320 kN that enables it to simulate extreme vehicle loading from wheel load of aircraft such as the Boeing 777, Airbus 340 or 380. The four-segmented loading plate of 300 mm or 450 mm diameter, cushioned with a thin rubber pad is used to transmit the load of falling mass over the pavement surface. It is provided with a swivel to accommodate uneven pavement surfaces while testing. The resulting deflections are measured using a series of sensors spaced according to the configuration, which can accommodate up to 15 deflection sensors. In this study, HWD device is configured to have ten active sensors spaced at 0, 200, 300, 450, 600, 900, 1200, 1500, 1800,

and 2100 mm from the centre of the load plate (IRC 115, 2014). The key features of the device include high repeatability, single-person handling, and quiet operation. Being easy to operate and based on point testing process, data collection at one location takes around 50 seconds, and up to 60 test points can be tested every hour. The temperature sensors record the air and pavement temperatures while testing. Distance measurement and Global Positioning System (GPS) are also provided. The unit is operated by means of a 12V DC electro-hydraulic system. It produces a half-sine shaped single impact load of duration 25-30 ms. The deflection measurement resolution is 0.1 micron with a relative accuracy of 1% ± 1 micron. The load is measured with an accuracy of 2% ± 0.3 kN.

Figure 6.5 depicts the working principle of HWD. The falling mass overloading plate temporarily deforms the pavement into a deflection bowl, whose deflections (D1 to D10) are measured at various radially outward points from the centre of loading plate. These sensors provide structural condition information of various pavement layers depending on their position with respect to the centre, as illustrated in the figure.

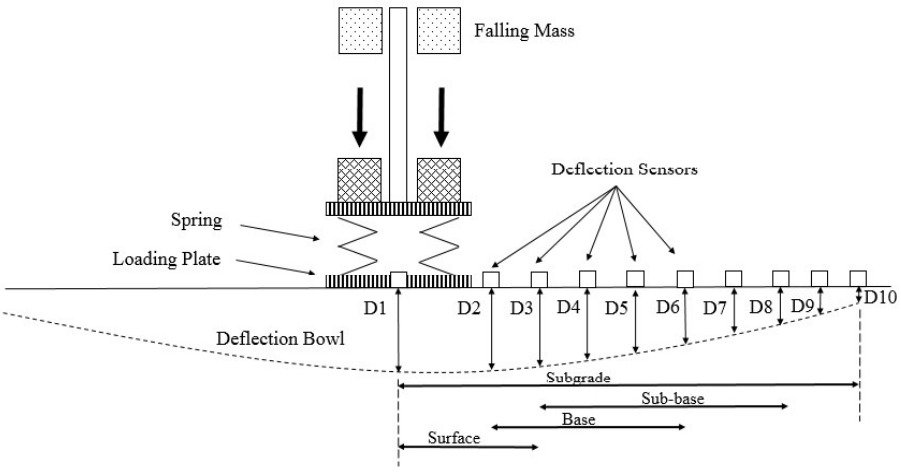

Figure 6.5. The working principle of HWD

6.4.2. Data collection and methodology

HWD deflection testing was conducted to estimate elastic moduli of pavement layers and subgrade, which in turn is a measure of their structural capacity. The testing was performed in

accordance with ASTM standards (ASTM D4694-09, 2015; ASTM D4695-03, 2015). The tests were conducted using a 300 mm diameter loading plate, at every 50 m interval and taken on longitudinal alignments at offsets of 3 m, 6 m and 9 m, both the sides of the runway centerline in a staggered manner and also at 20 m offset on shoulders. The measurements were done with three drops of mass, first being the seating load, and tests were performed at 438 locations. Pavement and air temperatures were recorded in conjunction with each test. The collected data was normalized, and corrections for seasonal moisture and temperature variations were applied. Pavement thickness information was collected using GPR. A limited number of core samples were also extracted from each homogeneous section, to verify thickness, check the subsurface material disintegration, if any, and ensure reliability in measurements and analysis. The HWD test has also been performed on the parallel taxiway, ET2, ET3 and ET5, and turn pads.

6.4.3. Data processing

Deflection data collected at the aforementioned test locations have been back-calculated using Dynatest software ELMOD 6 (Elmod, 2008). The forward analysis in ELMOD 6 is based on the theory of Odemark-Boussinesq transformed section. For back-calculation, deflection basin fit method is used in this study. Deflection basin fit method starts with an assumption of a set of moduli for the pavement structure and calculation of theoretical deflection bowl. The measured and calculated deflections are compared, and errors between them are assessed. Accordingly, the moduli in the structure suitably changed by increasing or decreasing it with a small amount (typically 10%). A good solution is obtained when an error in either of these deflection bowls is less than the original deflection bowl. This process is iterated to satisfy the prescribed limit of minimum standard error between the calculated and measured deflections. Apart from the estimation of layer moduli at each test point, calculation of Aircraft Classification Number (ACN) and Pavement Classification Number (PCN) have also been performed. The PCN module calculates PCN in accordance with the ACN/PCN method, as described in the International Civil Aviation Organization (ICAO) and Federal Aviation Administration (FAA) design manuals. The critical aircraft considered for ACN-PCN estimation in this study is Boeing B777-200 with aircraft weight of 298010 kg.

6.4.4. Results and discussion

The results obtained through HWD testing on the runway are presented in the form of deflection measurements using ten sensors, back-calculated layer moduli, and ACN-PCN classification, at various test locations. The layer thickness requirements were fulfilled by conducting GPR surveys which is covered under the next section.

6.4.4.1. Deflection measurements

Deflections of pavement surface represent their most probable structural condition. Higher pavement surface deflections indicate weaker pavement strength. The falling mass of HWD deforms the pavement into a deflection bowl in which central deflection is the highest. The variation of deflections measured by ten sensors of HWD (D1 to D10, refer Figure 6.5) along L3, L6, R3, and R6 (where L and R refers to left and right side of runway centerline; 3 and 6 represents 3 m and 6 m offset, respectively) are presented in Figure 6.6. The non-uniform variation of deflection shows varying strength of pavement structure. Higher deflection values are typically obtained at zones of 0.40 to 0.60 km, and 2.00 to 3.05 km, measured from '02' end of the runway. This gives an indication that these are weak zones, which has also been concluded from the results of the visual survey.

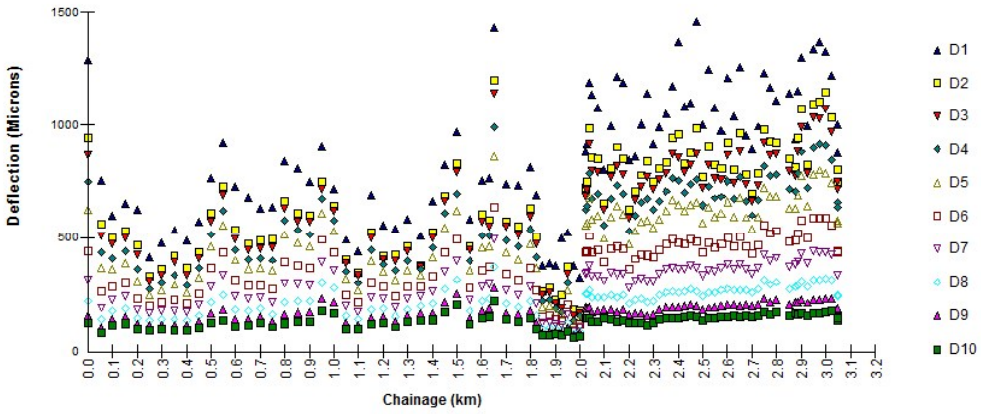

(a) Variation of pavement surface deflections along L3

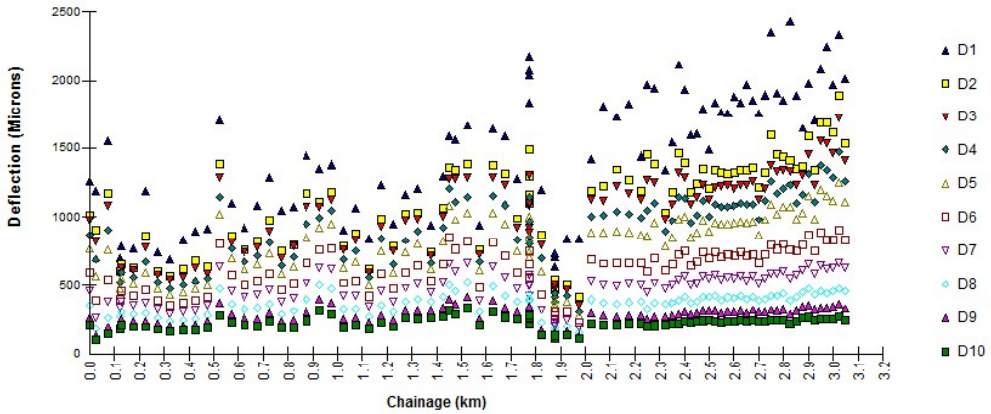

(b) Variation of pavement surface deflections along L6

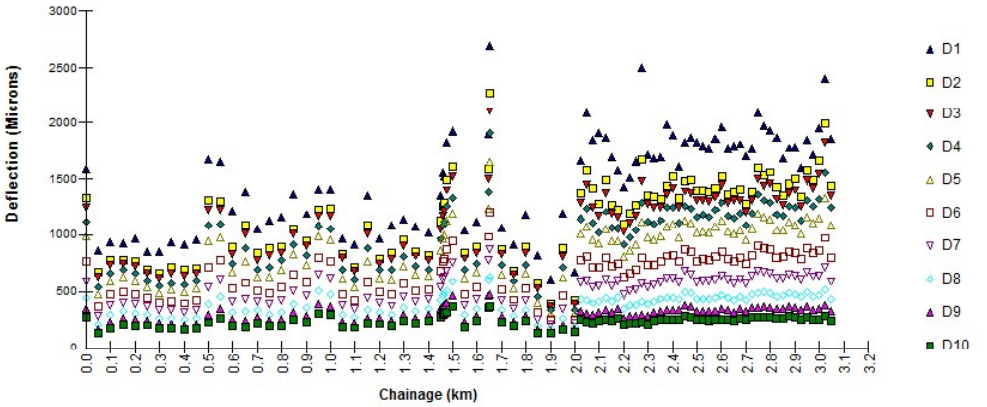

(c) Variation of pavement surface deflections along R3

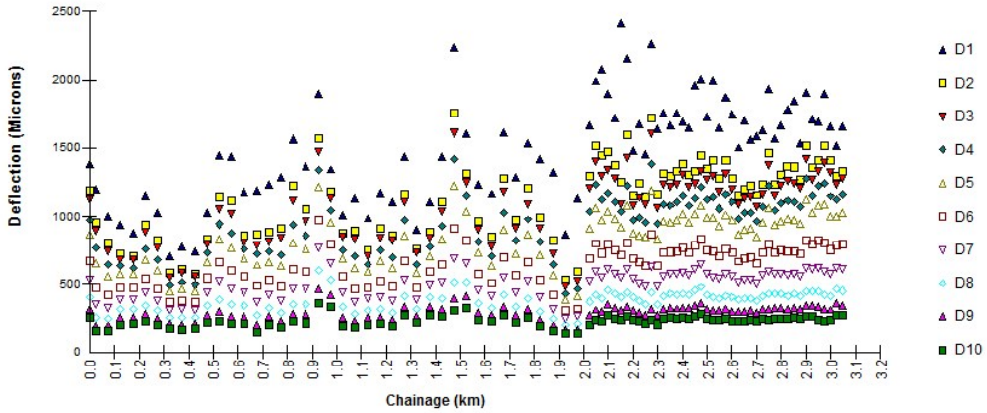

(d) Variation of pavement surface deflections along R6

Figure 6.6. Variation of pavement surface deflections along the runway

6.4.4.2. Layer moduli estimation

The modulus value of any structure is a measure of its stiffness. The higher values of modulus indicate that the material is stiffer and less likely susceptible to deformation under load. Therefore, it is crucial to consider the moduli value of pavement layers for assessing their current state. The back-calculation of all the deflection values, with suitable input seed moduli and using GPR data to input the layer thickness values, resulted in estimating the moduli of subgrade, base, and asphalt concrete layers. The longitudinal variation in moduli along the runway has been presented in Figure 6.7, which clearly demonstrates that higher moduli values indicate high strength of pavement layers at the locations with the lower deflections and vice versa. The zone 2.00 to 3.05 km can be observed to have either inconsistent or low moduli values. The results are found to be consistent with visual surveys, and other test results at these locations.

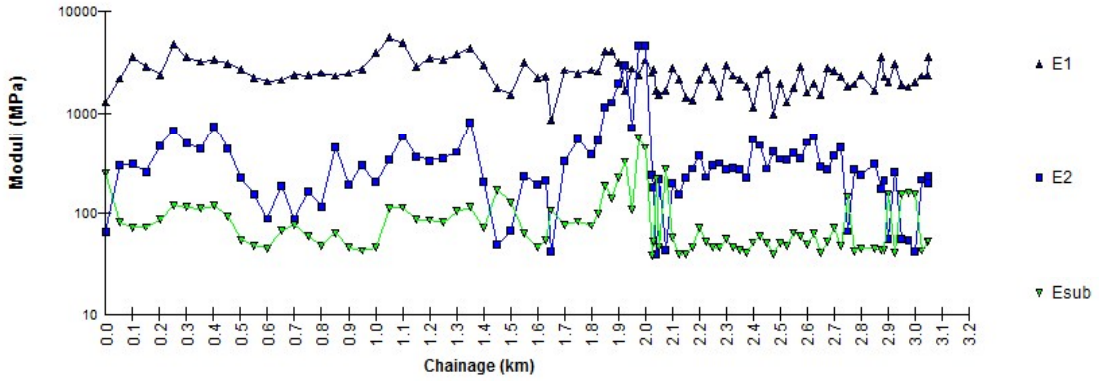

(a) Variation of pavement layer moduli along L3

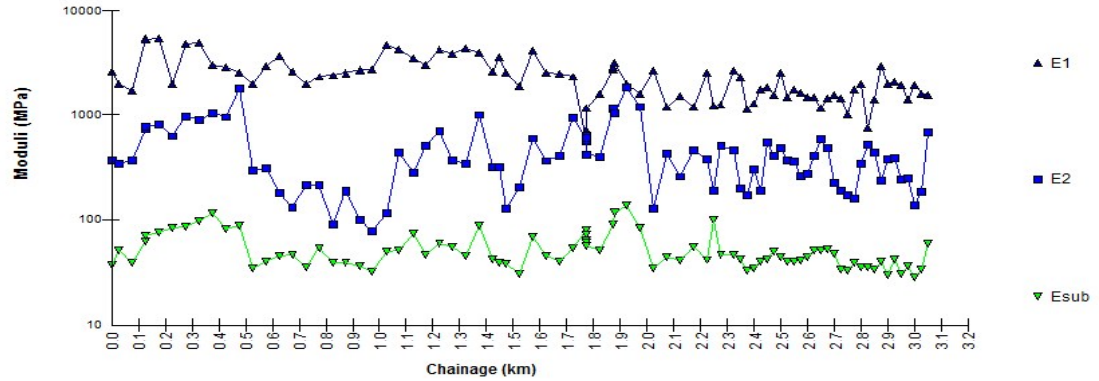

(b) Variation of pavement layer moduli along L6

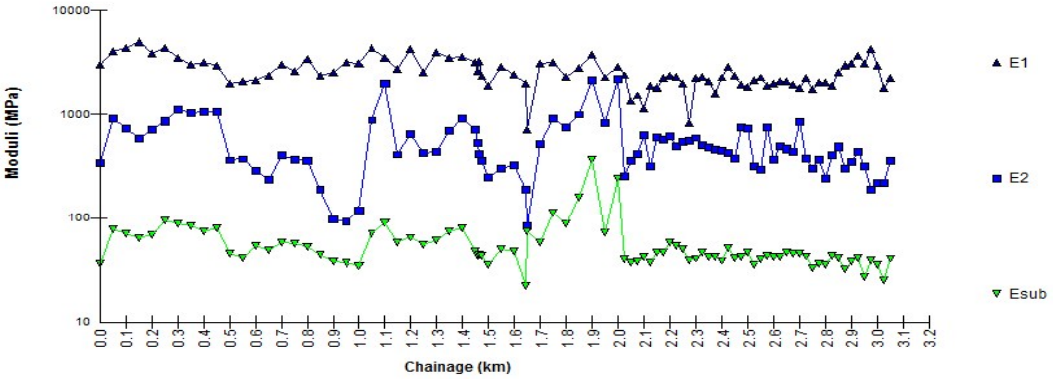

(c) Variation of pavement layer moduli along R3

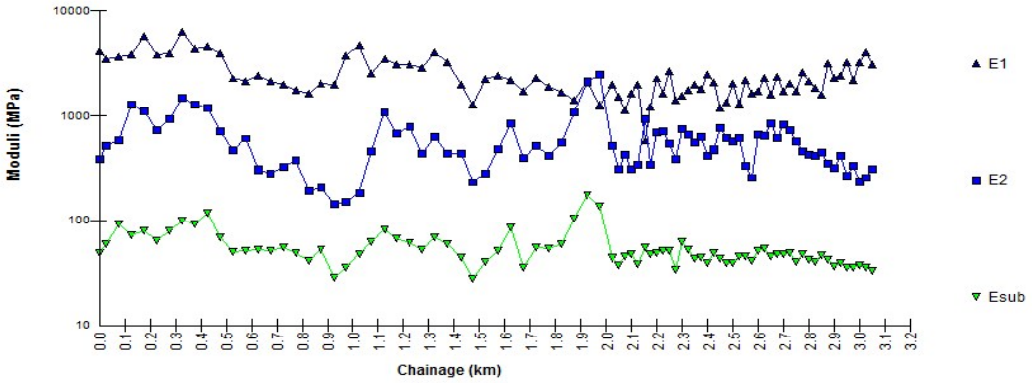

(d) Variation of pavement layer moduli along R6

Figure 6.7. Variation of pavement layer moduli along the runway

6.4.4.3. ACN-PCN classification

In accordance with ICAO, ACN/PCN method is used to classify aircraft's load rating and pavements' bearing strength. ACN is 'a number that expresses the relative effect of an aircraft at a given configuration on a pavement structure for a specified standard subgrade strength' (FAA, 2014b). It is a number on a continuous scale ranging from 0 and with no upper limit. The ACN is specific to a particular aircraft and does not depend on the number of operations or on the pavement structure apart from the subgrade category. The aircraft manufacturer provides the official computation of an ACN value. PCN is a number that expresses the load-carrying capacity of

pavement for unrestricted operations (FAA, 2014b). It depends on the expected number of load repetitions and pavement structure. The ratio of ACN and PCN is known as the structural index. ACN/PCN method is a way of rating airport pavements and assesses acceptable operations of aircraft. It is just a classification system and is not a design or evaluation method. It only deals with aircraft weighing in excess of 5,700 kg. It ensures that pavement can support an aircraft that has an ACN value equal to or less than its PCN value. More details of the method can be found elsewhere in the literature (FAA, 2014b).

Figure 6.8 shows the plots of ACN and PCN numerical value. The critical aircraft considered here was Boeing B777-200. It can be seen that at the locations where moduli values are lower, PCN numerical values are also less. From chainage 2.00 km to 3.05 km, it can be concluded that since this section was already in poor condition, as seen from deflection and moduli values, the PCN values over the entire section are lower as compared to other sections.

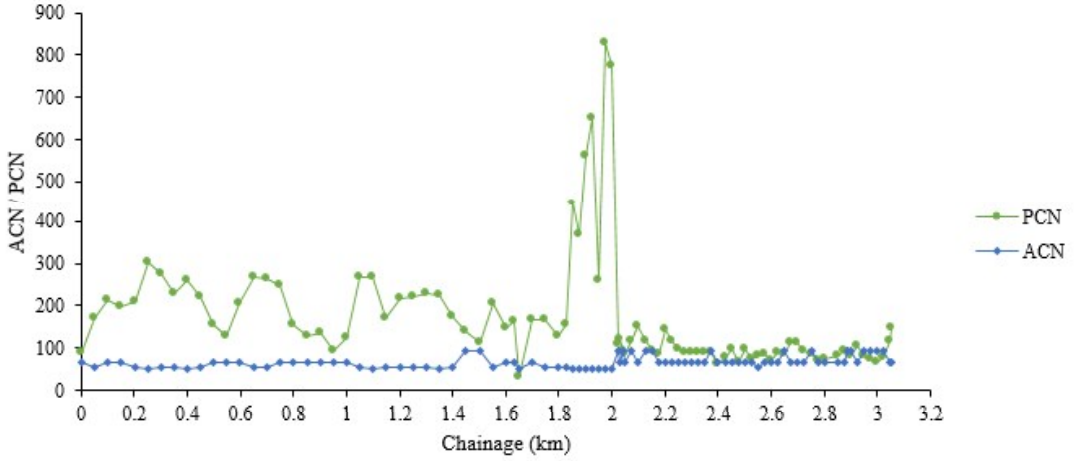

(a) Variation of ACN and PCN value along L3

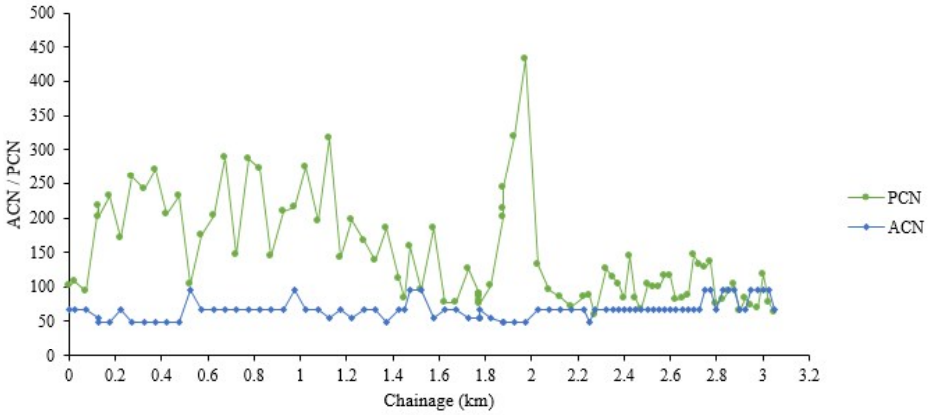

(b) Variation of ACN and PCN value along L6

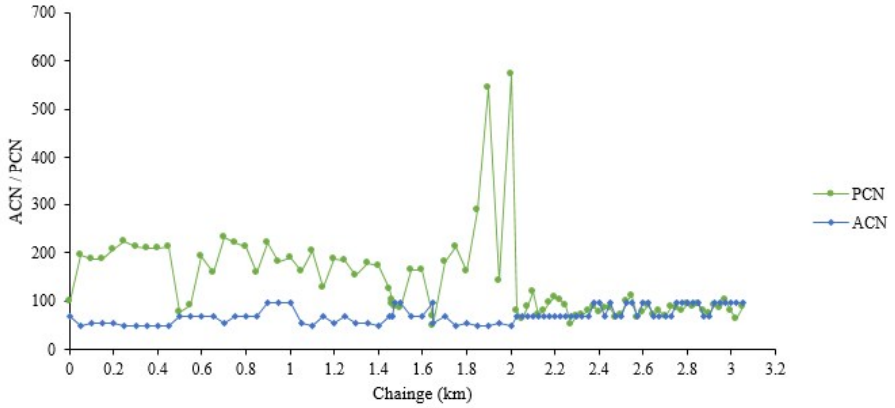

(c) Variation of ACN and PCN value along R3

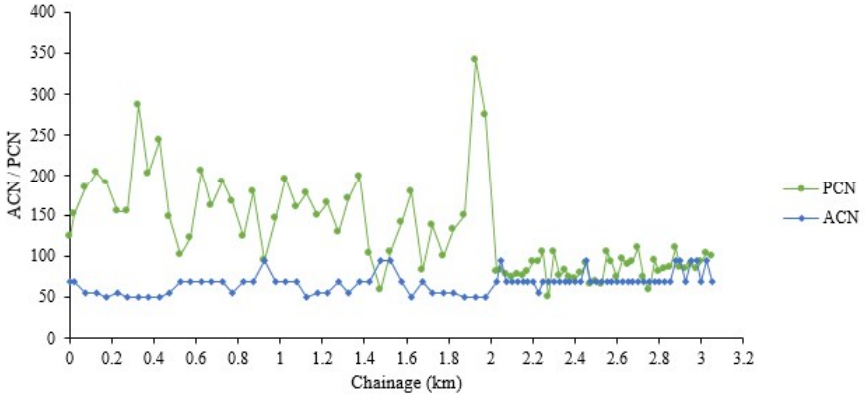

(d) Variation of ACN and PCN value along R6

Figure 6.8. Variation of ACN and PCN value along the runway

6.5. GPR testing

GPR tests have been primarily performed to collect the pavement layer thicknesses information about the airfield pavements, that is further used during the process of back-calculation for the estimation of layer moduli. In addition to this, the GPR scans also provide vital findings about subsurface conditions. The theory and details of GPR equipment are covered previously in Chapters 2 and 4, therefore, excluded from discussion in this chapter.

In the present case study, GPR surveys were conducted using two antennae of 1500 MHz and 400 MHz frequency along six parallel lines of runways and taxiways, and the data is analyzed in commercial software RADAN. The 1500 MHz antenna provided clear details at closer depth whereas details at greater depths were better captured by 400 MHz antenna. However, data captured from both the antenna were integrated to observe asphalt and base layer together and enhance the understanding of subsurface conditions. The profiles show deteriorated and settled pavement layers at many locations. The possible reasons could be contributed to the presence of voids, and moisture infiltration during monsoon season. These locations have eventually resulted in the loss of structural integrity of pavement owing to the lack of sufficient support at the base and subgrade. It should be noted that steps of data processing in RADAN software are already covered under Chapter 4, and hence, not repeated in this section.

6.5.1. Results and discussion

The results obtained through GPR testing on runway and taxiways are presented in the form of layer thickness measurements, GPR sectional profiles, and 3D views revealing subsurface condition and are summarized in the following sections.

6.5.1.1. Layer thickness measurements

Pavement layers are designed to a sufficient thickness to ensure that the imposed loads would not lead to the failure of the pavement structure. The designed thickness depends on subgrade conditions, and the weight and volume of the upcoming traffic. Layer thickness information is an important input for layer moduli calculations, and GPR is extensively used for this purpose. Additionally, measurements of layer thickness provide a preliminary indication regarding the

occurrence of any pavement distress, apparently seen by the change in its thickness value from the designed thickness. Nevertheless, the estimation of subsurface conditions from layer thickness values provide rather some rough idea. A thorough examination of GPR linescans provides detailed findings about the same.

GPR with 400 MHz and 1500 MHz antennae has been used to measure the thickness of pavement layers in this study. The survey has been conducted along six profiles parallel to the centerline of runway and at 3 m, 6 m and 9 m offset both sides. Figure 6.9 presents the longitudinal profile of runway pavement layer thicknesses (asphalt concrete layer: H1, base: H2, and subgrade), chainage-wise, along L3, L6, R3, and R6 (where L and R refers to left and right side of runway centerline; 3 and 6 represents 3 m and 6 m offset, respectively). The thickness of the first layer (H1) as measured from GPR, varies from 234 mm to 689 mm, and that of the second layer (H2) varies from as low as 181 mm to as high as 1717 mm. The observation gives an indication of poor pavement strength, and the possible presence of subsurface voids, leading to highly varying thickness since it is expected that strong pavement would be sufficiently and uniformly compacted with a more or less constant thickness of its layer.

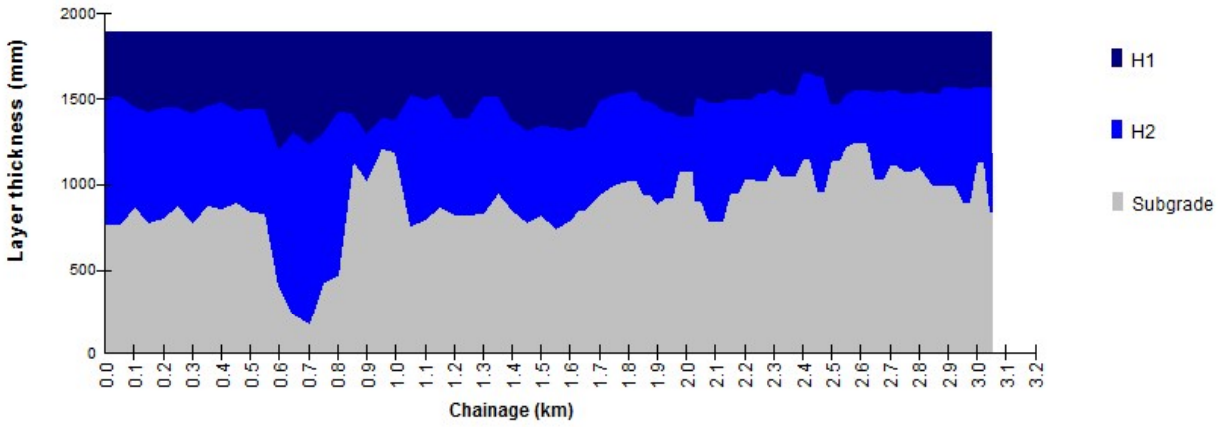

(a) Variation of pavement layer thicknesses along L3

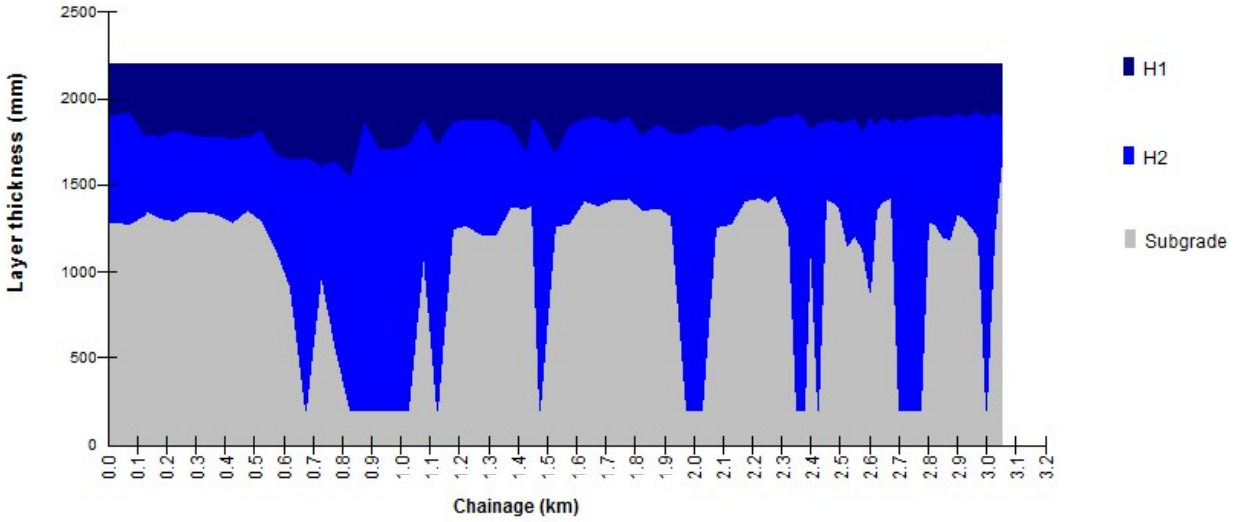

(b) Variation of pavement layer thicknesses along L6

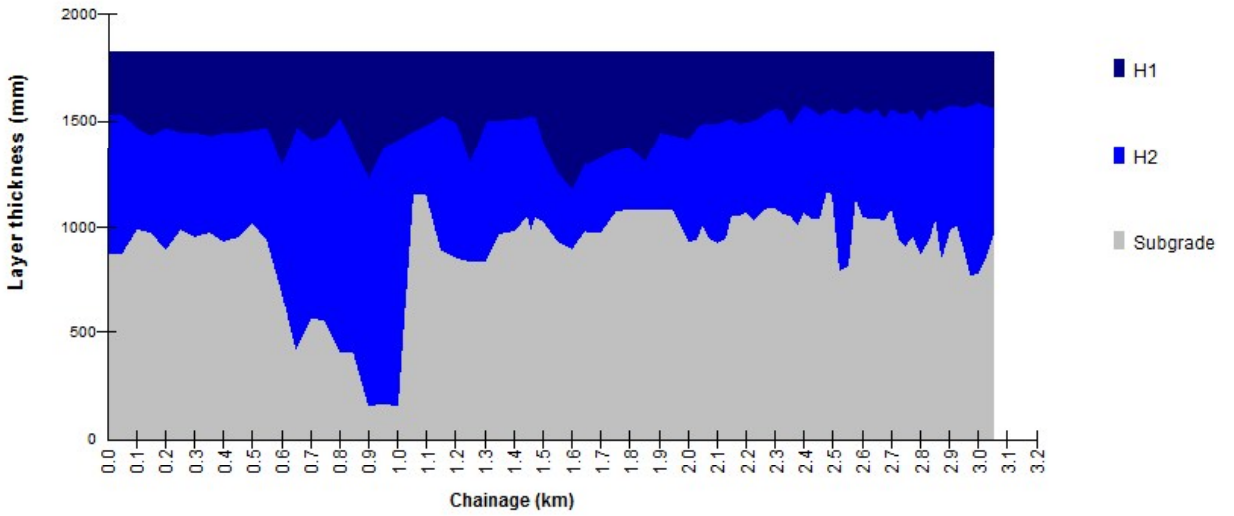

(c) Variation of pavement layer thicknesses along R3

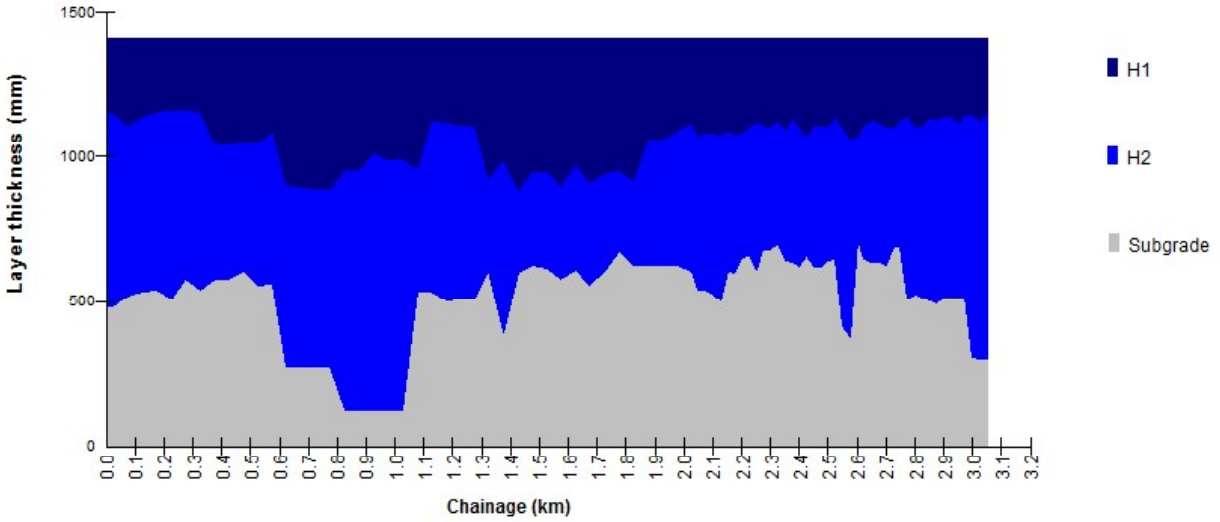

(d) Variation of pavement layer thicknesses along R6

Figure 6.9. Variation of pavement layer thicknesses of the runway

From all figures, it can be seen that at around 0.56-1.10 km, there is an abrupt increase in the thickness of the second layer which is an indication of weak or settled subgrade. Further performing NDT at this location has verified the existence of poor subgrade conditions. Figure 6.10 shows a part of the GPR sectional profile taken with 400 MHz antenna along L6. The pavement layers can be seen clearly and settlement of the layers can be observed at chainage of 1.196 km (encircled). This is in agreement with the sudden increase in layer thickness at this particular location as observed from Figure 6.9b.

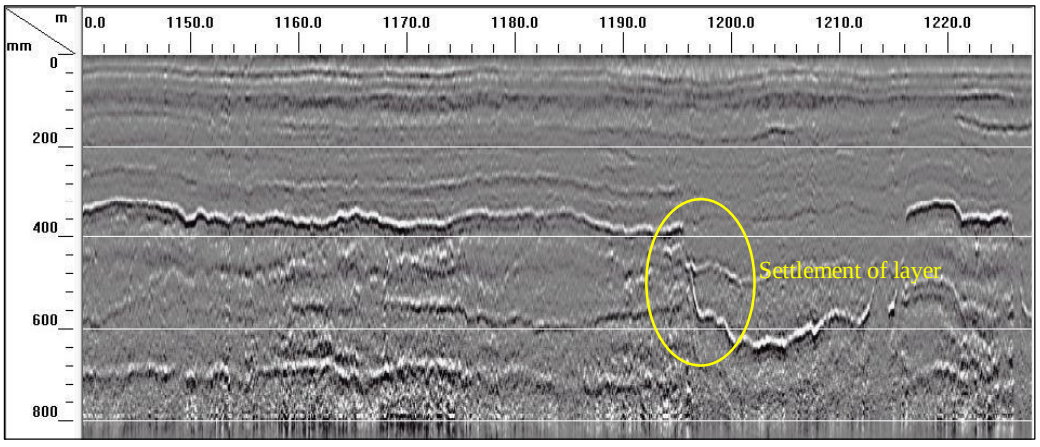

Figure 6.10. Sectional profile showing settlement of pavement layers

6.5.1.2. GPR linescans

Detailed examination of GPR sectional profiles taken along the entire 3.05 km length of the runway revealed the reasons for distresses identified during the visual surveys in section 6.3 and high surface deflections reported in section 6.4 of this chapter. A GPR profile using 1500 MHz antenna along L3 from '02' end of the runway is shown in Figures 6.11 and 6.12. The bottom of the asphalt layer can be seen clearly, as indicated in Figure 6.11. Settlement of 10 cm at 95 m chainage from '02' end is also noticed. Reflection of heavy deterioration can be witnessed in Figure 6.12.

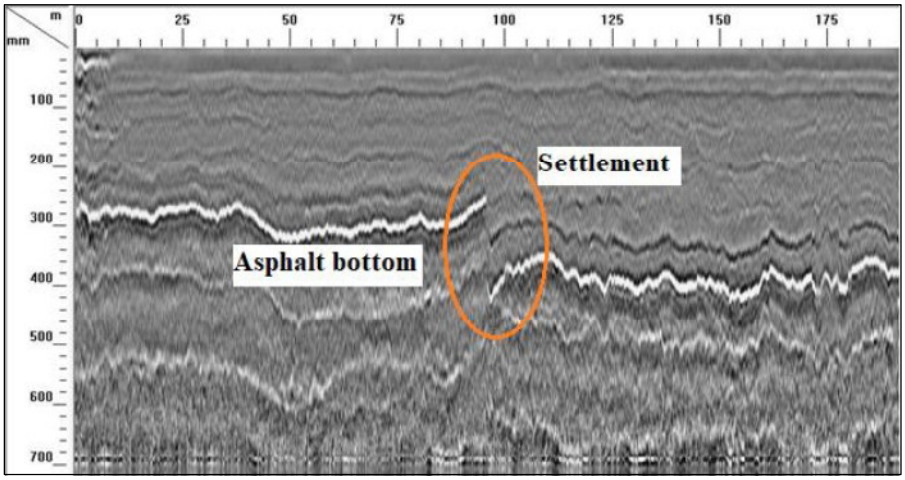

Figure 6.11. Sectional profile of runway showing asphalt layer and its settlement

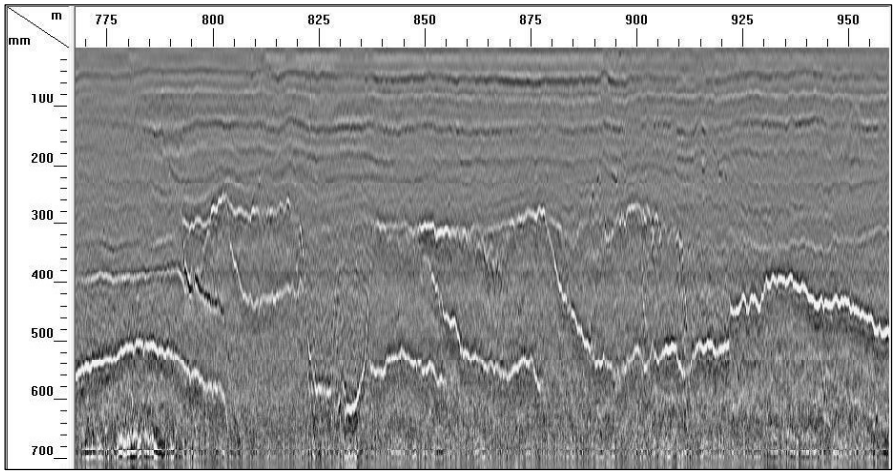

Figure 6.12. Sectional profile of runway showing inconsistent reflections indicative of deterioration

Figure 6.13 presents GPR profile along L6 from '02' end of the runway. The data from 1500 MHz and 400 MHz antennae are integrated to apparently spot asphalt and base layer. About 30 cm settlement of base layer can be observed from 364 m to 372 m distance. Heavy deterioration and settlement are observed from Figures 6.14 and 6.15.

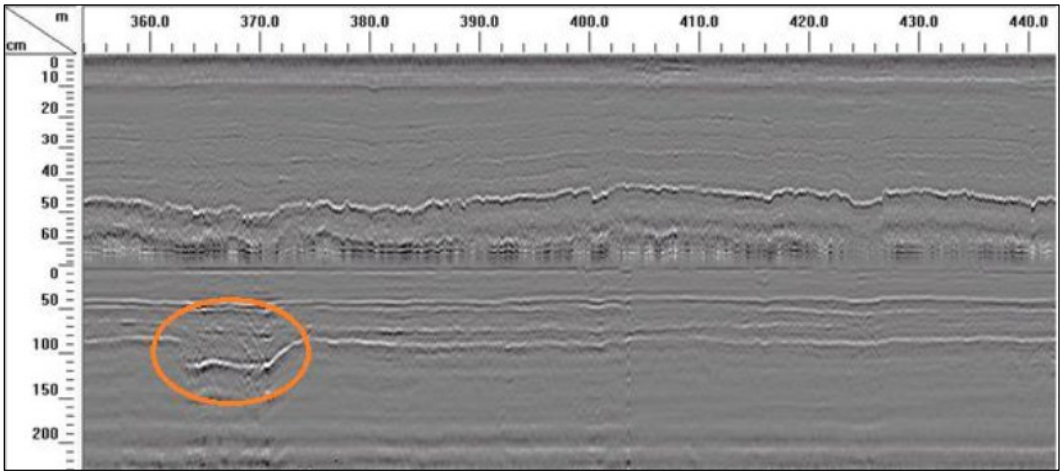

Figure 6.13. Sectional profile of runway showing settlement of base layer

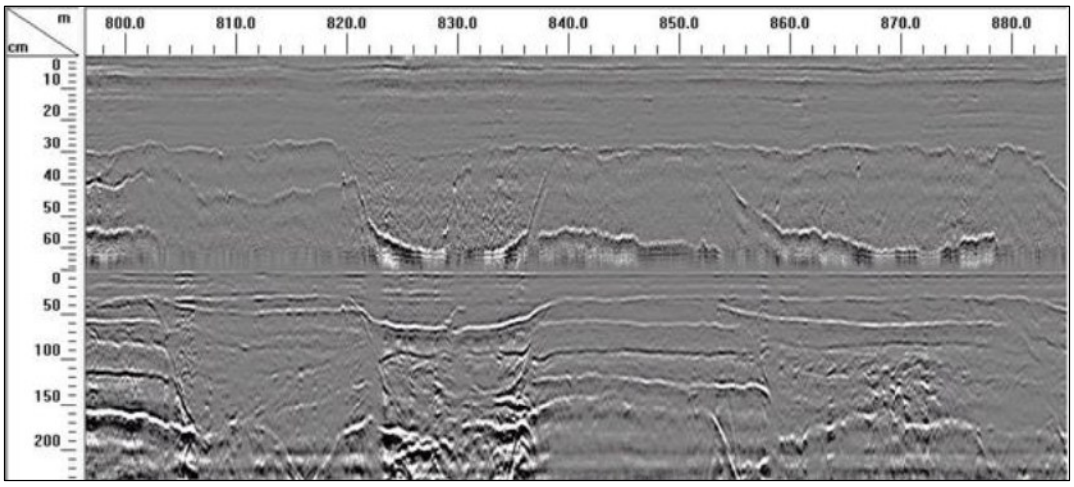

Figure 6.14. Sectional profile of runway showing settlement of layers and their deterioration

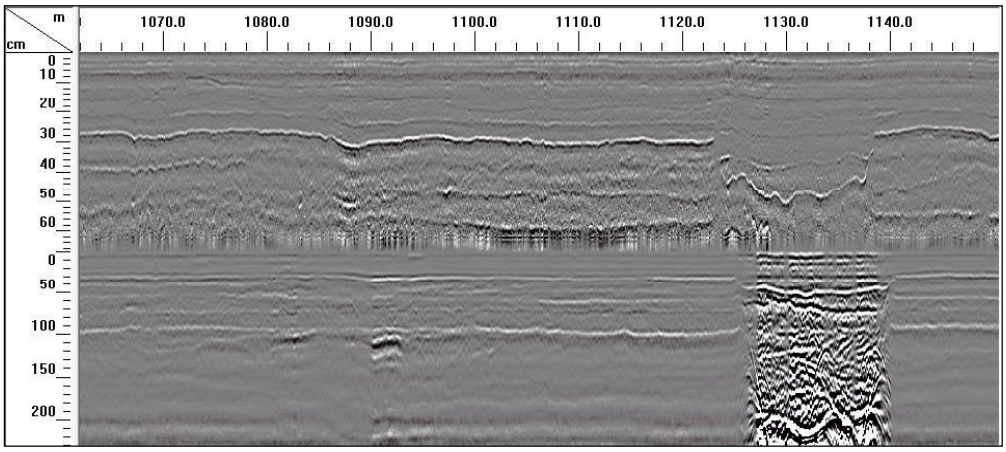

Figure 6.15. Inconsistent reflections in sectional profile of runway due to settlement of layers and their deterioration

Figure 6.16 shows the settlement of layers in 1500 MHz and 400 MHz integrated GPR profile taken along R6 from '02' end of the runway.

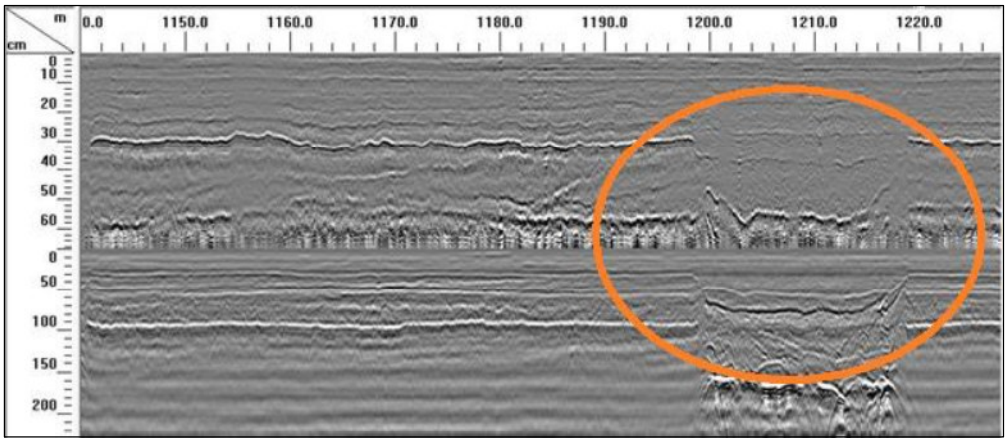

Figure 6.16. Sectional profile of runway showing settlement of layers

Similar surveys were also conducted on parallel taxiways and exit taxiways. Figure 6.17 shows the profile of ET1 along L3 from '02' end of runway taken through 400 MHz antenna.

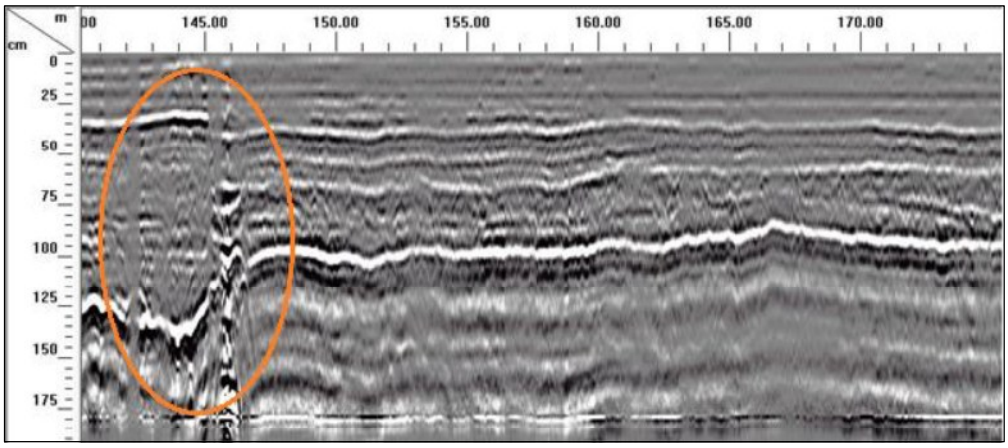

Figure 6.17. Sectional profile of ET1 showing layer settlement

6.5.1.3. 3D view from GPR linescans

The GPR linescans captured using 400 MHz antenna were then used to create a plan view in 3D. This facilitated a different perspective to the presentation of results where the entire runway could be seen at once. The colours represent the intensity of the degree of deterioration, with stronger reflections representing higher deterioration, as depicted in Figure 6.18. Figure 6.19 present the 3D views of the runway at different depths. It can be seen that the reflections become stronger with increasing depth. Also, more reflections are seen in the last one km section of the runway, indicating its heavy deterioration. These findings are consistent with the results obtained from HWD tests and visual surveys.

Less deterioration  **High deterioration**

Figure 6.18. Color intensity scale used in 3D views

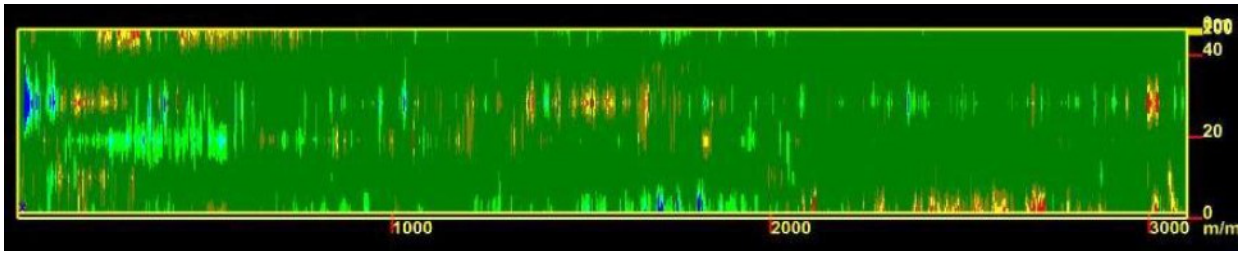

(a) 23 cm

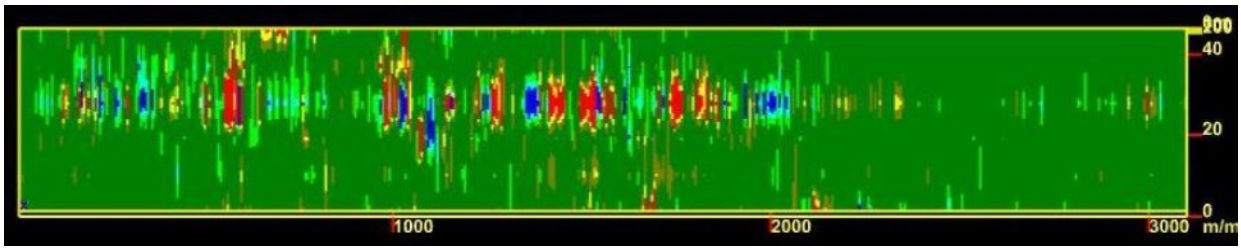

(b) 47 cm

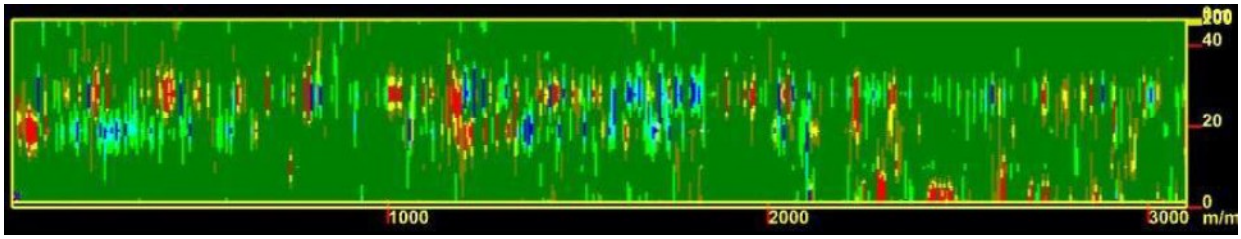

(c) 71 cm

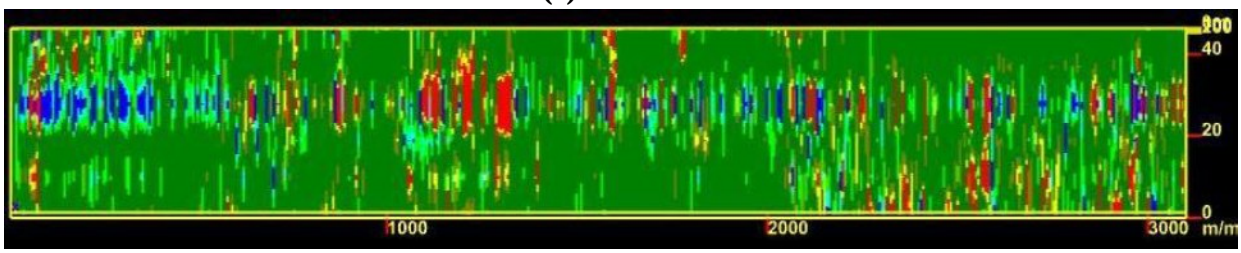

(d) 95 cm

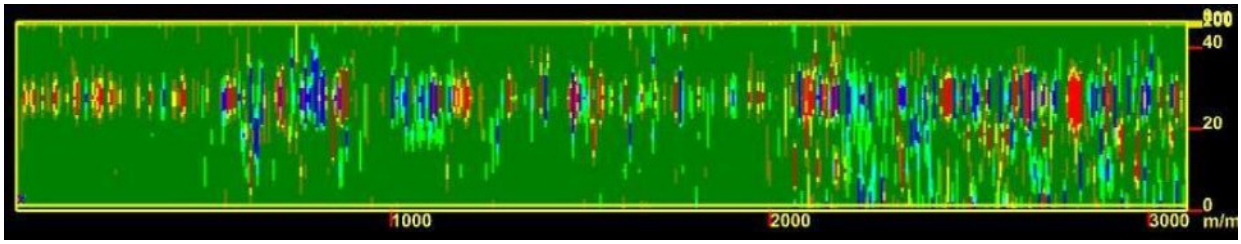

(e) 120 cm

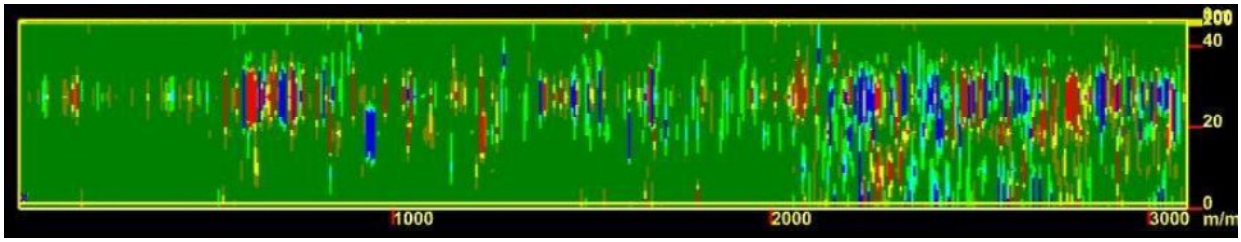

(f) 145 cm

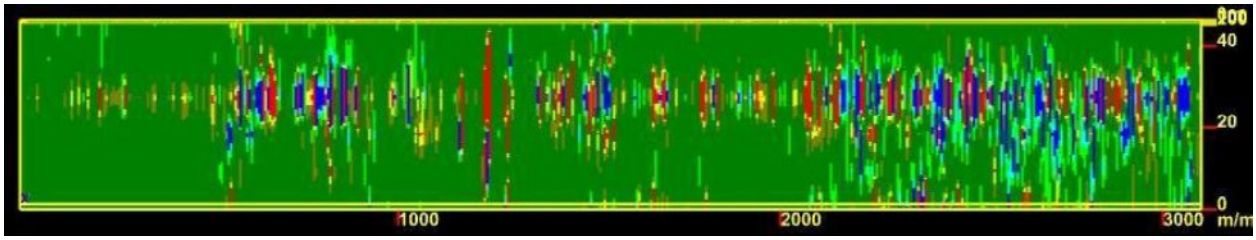

(g) 170 cm

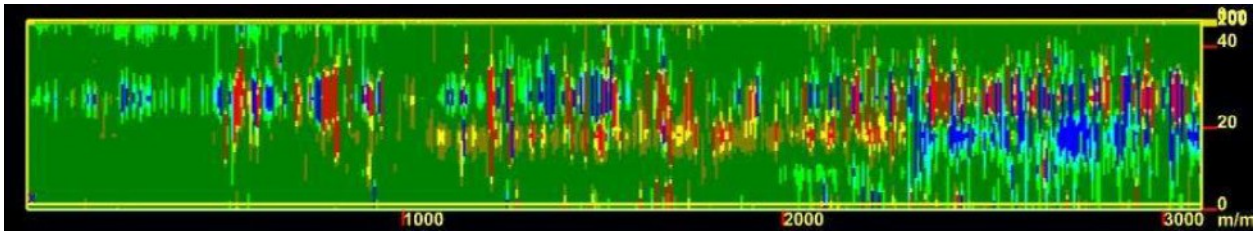

(h) 190 cm

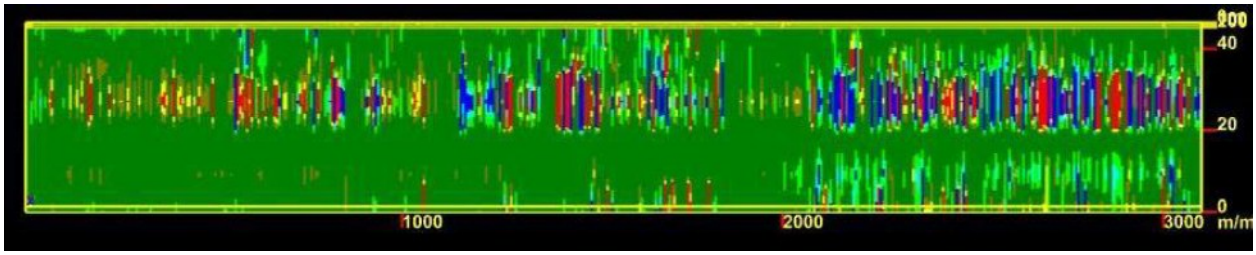

(i) 215 cm

Figure 6.19. Depth slice of runway at various depths

6.6. Concluding remarks

This chapter summarizes the results of uncontrolled field investigations performed on airfield pavements using visual inspections, HWD and GPR tests. A limited number of NDT devices could be used due to the non-availability of other equipment. Various vital conclusions can be drawn from the field examination conducted in this study. As such, all the investigation methods reported that the airfield pavement network is in poor health condition which demands adequate M&R applications.

The impact of structural deficiency of pavements adversely affecting the functional and operational conditions of pavements can be clearly understood by deeply observing the outcomes from all three studies (visual surveys, HWD tests and GPR tests). The distresses appearing on the

pavement surface as identified from the visual surveys, reflected poor structural capacity as recognized from higher HWD deflections and eventually, both of these were occurring due to deficiency in subsurface support conditions which was unfolded by GPR scans. Although, none of the method as standalone provided the complete representation of the existing condition of airfield pavements, however, the combination of these methods have complimented well to report the major findings on pavement condition in this case study.

Visual surveys are pioneer in identifying and demarcating the areas with a higher degree of pavement deterioration that can be meticulously examined using different techniques. However, these surveys often portray a vague depiction of the pavement condition which demands a strong basis of reliable assessments to take sound M&R decisions. Also, manually conducting these surveys for large areas is challenging, and not feasible. Using automation in performing visual surveys would offer more efficiency and ease. Moreover, monitoring pavement health using NDT technologies to investigate its degradation at early stages is anticipated. In this context, HWD was notable for estimation of the structural capacity of pavements, and to some extent, it can aid in delineating zones with structural disintegration. Nevertheless, to ensure consistency in findings, it is desirable to be followed by other NDT technologies. Application of GPR at the test locations has shown excellent capabilities of subsurface imaging, and the linescans have provided a significant information about the subsurface deterioration, as predicted from HWD tests and visual surveys. Integration of results from two different antennae assisted to precisely notice the details closer to the surface as well as the deeper ones. Employing advanced algorithms for data analyses may fetch better results.

Furthermore, apart from demonstrating the utility of NDT techniques under uncontrolled field conditions, these testing results have served as a crucial input in the process of formulating decision-support system for taking maintenance decisions, as discussed in the next chapter.